Organic π-Conjugated Trimers as Fluorescent Molecules for Colorful Electroluminescence †

Yanhong Deng, Yifei Wang, Zhesheng Chen, Bo Xu, Jinjiang Wang, Eric Cloutet, Xiaojiao Yuan, Hengyang Xiang

Organic π-Conjugated Trimers as Fluorescent Molecules for Colorful Electroluminescence†

Yanhong Deng,[‡a] Yifei Wang,[‡b] ZheshengChen, [b] Bo Xu, [b] Jinjiang Wang, [a] Eric Cloutet, [c] XiaojiaoYuan[*c] and Hengyang Xiang[*b]

[a]College of Physics and Electronics Engineering, Hengyang Normal University, Hengyang, Hunan 421002, P. R.China

[b]MIIT Key Laboratory of Advanced Display Materials and Devices, Institute of Optoelectronics & Nanomaterials, School of Materials Science and Engineering, Nanjing University of Science and Technology, Nanjing, Jiangsu 210094, P. R.China

[c]Laboratoire de Chimie des Polymères Organiques (LCPO-UMR5629), Université de Bordeaux, F-33607 Pessac, France

[*] Corresponding authors and E-mail addresses:xiang.hengyang@njust.edu.cn(H. Y. Xiang), xyuan@iciq.es(X. J. Yuan)

[‡]These authors contributed equally to this work.

Abstract: Organic fluorescent emitters based on π-conjugated small molecules show tremendous potential in display, lighting, and bio-imaging. However, these emitters face challenges of aggregation-caused quenching and limitations of color range caused by synthetic complexity and undesirable efficiency and quantum yield. In this work, by using quinoxaline/2,1,3-benzothiadiazole as central electron acceptors, and employing carbazole/thiophene/3,4-ethylenedioxythiophene as terminal electron donors, a series of π-conjugated fluorescent trimers with very low molecular weights (M_w = 294 ~ 466) were designed and synthesized. Modulating the molecular structure through the incorporation of distinct electron donor and acceptor moieties, broad spectral tuning from blue to red in the π-conjugatedtrimerswere obtained. Application of these conjugated trimers as emitting layers in electroluminescent devices, particularly organic light-emitting diodes (OLEDs), exhibits high brightness and color-tunable electroluminescence electroluminescence (EL) peak from 528 to 605 nm). The meticulously optimized device demonstrates excellent performance with a high brightness of 3857.19 cd m^{-2}, and an external quantum efficiency (EQE) of 2.29%. These π-conjugated trimers, synthesized by simple synthesis process, present a viable avenue for low-cost luminescence applications in lighting and display.

Keywords: π-conjugated trimers, D-A-D, solution processing, organic light-emitting diode, multicolored emission, spectral tunability

1. Introduction

Organic light-emitting diodes (OLEDs) exhibiting visible and white electroluminescence (EL) have demonstrated significant potential for applications in displays and solid-state lightings.[1-4] However, the polymer or small molecule emitters widely used in OLED, exhibit limited color range, efficiency and quantum yield. Besides, intricate structures and synthetic complexity result in high cost in materials and hindering the application of OLEDs. Small molecules with donor (D)-acceptor (A) molecule structures may promote the emission efficiency by facilitating injection and transportation of holes.[5-7] Meanwhile, emitting layer with small molecular in OLED device can effectively reduce the luminescence quenching phenomenon caused by the interaction between molecules and electron coupling.[8, 9] For instance, small

molecule emitters with wavelengths of 496 nm and 581 nm can be obtained through the attachment of cyano-functional groups to the main chain of the multi-resonant thermally activated delayed fluorescent (MR-TADF) molecule, which caused a red-shifted emission with 33.7% of the maximum external quantum efficiency (EQE) and a full width at half maximum (FWHM) of 49 nm in its OLED.[10] Moreover, substituted aza-boron Dipyridylmethene (aD) compounds are demonstrated as fluorescent dopant emitters for blue OLED (photoluminescence (PL) peak from 400-500 nm) with a maximum EQE of 3.5% at the electroluminescence peak of 445 nm, exhibiting low efficiency roll-off.[11] Also, a new oligo(p-phenylene ethynylene)-based small molecule as electroluminescence peaks of 452 nm in a deep blue A-π-D-π-A emitter with a maximum EQE of 7.06% and a maximum current efficiency of 5.91 cd A^{-1} was achieved. [12] These studies illustrate the feasibility of achieving light emission from small molecules by fine-tuning the luminescent component, all while maintaining a low molecular weight and a simple structure. Therefore, the main objective is to simplify the molecular structure and refine molecule design to create high-quality organic small molecule emitters.

However, achieving red, green, blue and complete visible luminescence for illumination and displays is still challenging.[13, 14] Reducing the molecular weight and simplifying the luminescent structure while maintaining spectral tunable luminescence is crucial for promoting the affordability of small molecules and their applications in OLEDs.[15-20] A series of fluorescent ultrasmall molecules with low molecular weights and large Stoke shifts by modifying diacetyl phenylenediamines (DAPAs) were obtained a wide range of spectral modulation (PL peak from 471 ~ 618 nm) by substituting same or different groups in the para-position of the benzene ring and among these molecules.[4] m-DAPA showed high-performance red emission with an extremely low molecular weight of 192.

To achieve broad spectral modulation of fluorescent small molecules, an essential strategy is to integrate two distinct fluorescent groups into a molecule with a D-A-D' or A-D-A' structure, transforming dominant chromophores.[21-23] Quinoxaline and 2,1,3-Benzothiadiazole are commonly used in red and near-infrared (NIR) emitters due to their strong electron acceptor capabilities.[24-33] For example, carbazole and thiophene exhibit deep highest occupied molecular orbital (HOMO) energy levels, and when paired with acceptor units featuring relatively high lowest unoccupied molecular orbital(LUMO) energy levels, which facilitates charge transfer from the donor to the acceptor, resulting in a blue shift of the spectrum.[34-37] In contrast, the conjugation property of 3,4-Ethylenedioxythiophene coupled with its high HOMO energy level, facilitates a red-shift in the spectrum of the D-A-D molecule towards longer wavelengths.[38, 39] Consequently, these molecules can be structurally modified to alter the energy level, enabling controlled luminescence band emission. Additionally, these groups extend the conjugation system within the structure of D-A-D small molecules, augment intermolecular charge transfer and interactions, and enhance the efficiency of charge transfer, ultimately improving the luminescence performance of fluorescent small molecules.

Hence, in this work, a series of fluorescent small molecules are constructed, incorporating terminal electron donor carbazole, thiophene, 3,4-ethylenedioxythiophene and central electron acceptor quinoxaline and 2,1,3-benzothiadiazole moieties, respectively. The interaction between A and D leads to tunable luminescence in the fluorescent small molecules, covering the illumination spectrum from sky blue to orange red. Subsequently, OLED devices were assembled, using a set of ultrasmall molecules as emitting layers, yielding electroluminescence peaks at 528 nm, 539 nm, 585 nm and 605 nm with a maximum EQE of 2.80% and a brightness of 3500 cd m^{-2}.Notably, the fabrication process employed

a solution-based method with a straightforward structure configuration, offering advantages in terms of cost reduction and promoting commercialization.

2. Experimental section

2.1 Materials

Poly(N-vinyl carbazole) (PVK), 1,3-Bis(5-(4-(tert-butyl)phenyl)-1,3,4-oxadiazol-2-yl)benzene (OXD-7), poly(3,4-ethylenedioxythiophene)polystyrene sulfonate (PEDOT:PSS) and 1,3,5-Tris(1-phenyl-1H-benzimidazol-2-yl)benzene (TPBi) were purchased from Xi'an Yuri Solar Co., Ltd. 4,7-dibromo-2,1,3-benzothiadiazole, 2-(tributylstannyl) thiophene, 9H-carbazole-2-boronic acid pinacol ester, 5,8-Dibromoquinoxaline, EDOT boronic acid pinacol ester, K_2CO_3, PEPPSI^{TM}-IPr, $PdCl_2(PPh_3)_2$ were obtained from Sigma-Aldrich. All reagents were used as received without further purification.

2.2 Emitter layer solution

PVK, OXD-7 and organic small molecules were dissolved in DMSO solution to prepare a solution of 10 mg/ml. Afterwards, PVK was doped with OXD-7 in the ratio of 7:3 as the hole transport layer (HTL) solution. The fluorescent small molecule solution was subsequently mixed with the HTL solution at 12 wt% to obtain the solution of the emitting layer (EML).

2.3 Device fabrication

Ethanol and acetone were used to clear the ITO-coated glass substrate by ultrasound, and UV treatment was performed for 15 min. Subsequently, the PEDOT: PSS solution was spin coated on the ITO glass substrate at 3000 rpm for 45 s, and heated at 145 °C for 15 min, and then, EML was spin-coated on it in a glove box in a N_2 environment at 3000 rpm for 30 s, and heated at 120 °C for 15 min. After spin-coating, it was placed in a high vacuum thermal evaporation coating system, and TPBi (30 nm) and LiF/Al (5 Å/100 nm) were deposited under a vacuum of about 2×10^{-4}Pa.

2.4 Characterization measurements

Ultraviolet Photoelectron Spectroscopy (UPS) was performed by PHI 5000 Versa Probe III with He I source (21.22 eV) under an applied negative bias of 9.0 V. The PL spectrum of the QDs was obtained using a spectrometer (Cary Eclipse, Agilent, Austria). The UV–vis light absorption spectrum was obtained by Shimadzu UV-3150 UV–vis–NIR spectrometer. The characteristics of LEDs were measured by a LED test system (Everfine Photo-E-Info Co., Ltd.), which was mainly composed of Keithley 2400 light source instrument and Konica Minolta CS-2000 spectrometer.

3. Results and discussion

3.1 Small molecular design

Fluorescent small molecule emitters are often designed using molecules with D-A-D' or A-D-A' structures because of their tunable molecule structures, enabling the preparation of fluorescent emitters with a broad spectral coverage by transforming different dominant chromophores.[40] Based on this design approach, we utilized quinoxaline and 2,1,3-benzothiadiazole as central electron acceptors to create a series of ultra-small molecular weight fluorescent emitters. By modifying the fluorescent groups at both ends, such as incorporation of carbazole, thiophene and 3,4-ethylene di-oxythiophene as terminal electron donors, four fluorescent small molecules (**B1**, **B2**, **Q1**, and **Q2**) were obtained to achieve luminescence modulation at low molecular weights (Fig. 1 and Fig. S9.).

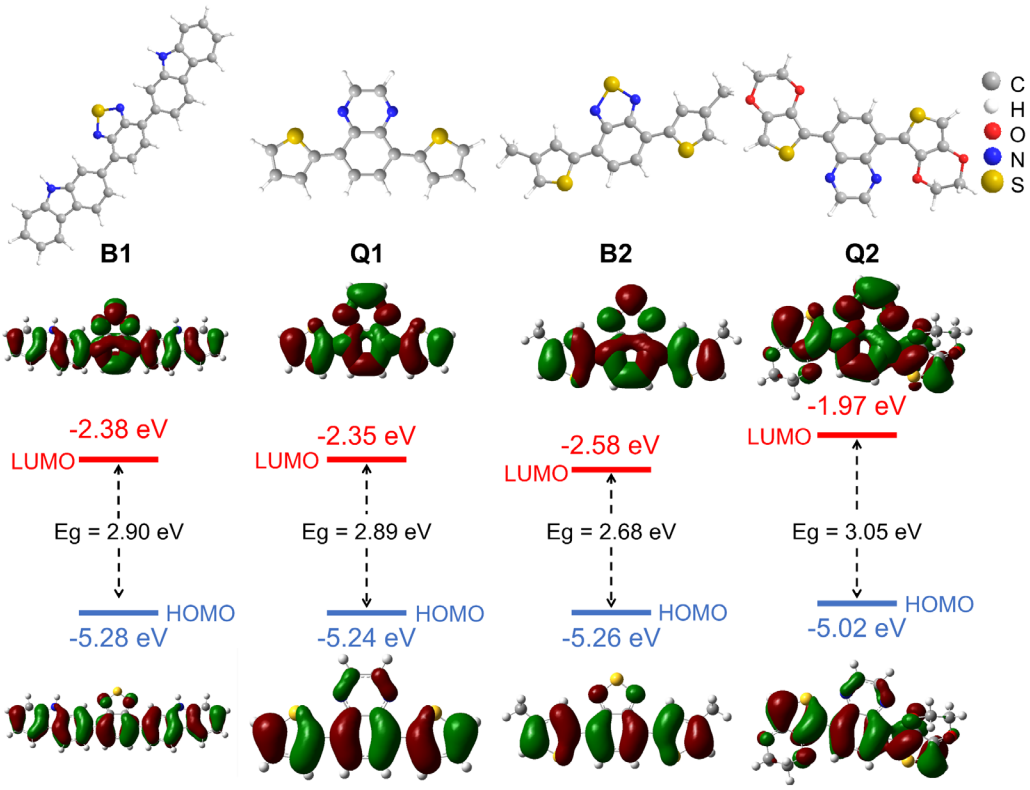

Fig.1. Molecular structures, HOMO/LUMO energies and orbitals of **B1**, **Q1**, **B2**, and **Q2**.

The corresponding synthetic routes are illustrated in Scheme S1-S4, Fig. S1-S8 and Scheme S1-S4. Thermogravimetric analysis (TGA) in Fig. S10. shows that the decomposition temperatures of the four small molecules B1, Q1, B2, and Q2 are 398.8°C, 293.6°C, 201.3°C, and 105°C, respectively. These relatively high decomposition temperatures ensure stability during the device fabrication process. To enhance processability and broaden spectrum tunability, various groups were attached to 2,1,3-benzothiadiazole and quinoxaline, ensuring solution processability while maintaining an exceptionally small molecular weight. Density functional theory (DFT) was carried out by Gaussian 09 program with B3LYP/6-31G(d) basis sets to investigate the frontier molecular orbitals (FMOs) and the highest HOMO/lowest LUMO levels of 2,1,3-benzothiadiazole/quinoxaline derivatives (i.e., **B1**, **Q1**, **B2**, and **Q2**). As shown in Fig. 1, all the molecules showed significant localized excited states. Due to the introduction of S and N elements in the acceptor units of these molecules, their HOMO-LUMO produced a little separation and exhibited better charge transfer (CT) properties.

3.2 Optical properties

The optical properties of **B1**, **Q1**, **B2**, and **Q2** in solutions were shown in Fig. 2a-d and Fig. S11-S13. All these small molecule emitters give bright emission with the emitting peak values ranging from 535 to 603 nm. **Q2** exhibited orange-red emissions with a PL peak at 603 nm, while Q1, B1 and B2 presented

excellent yellow-green luminescence properties with an emitting peak of 535, 547 and 559 nm, respectively. Meanwhile, the absorption spectra of the small molecules exhibit less overlap with their emission spectra, indicating a larger Stoke shift, which effectively reducethe internal filtering effect and leads to a higher luminescence efficiency. As shown in Figure S13, the fluorescence lifetimes of B1, Q1, B2, and Q2 are 6.39 ns, 12.48 ns, 13.25 ns, and 11.65 ns, respectively, confirming that these are all fluorescent small-molecule materials.

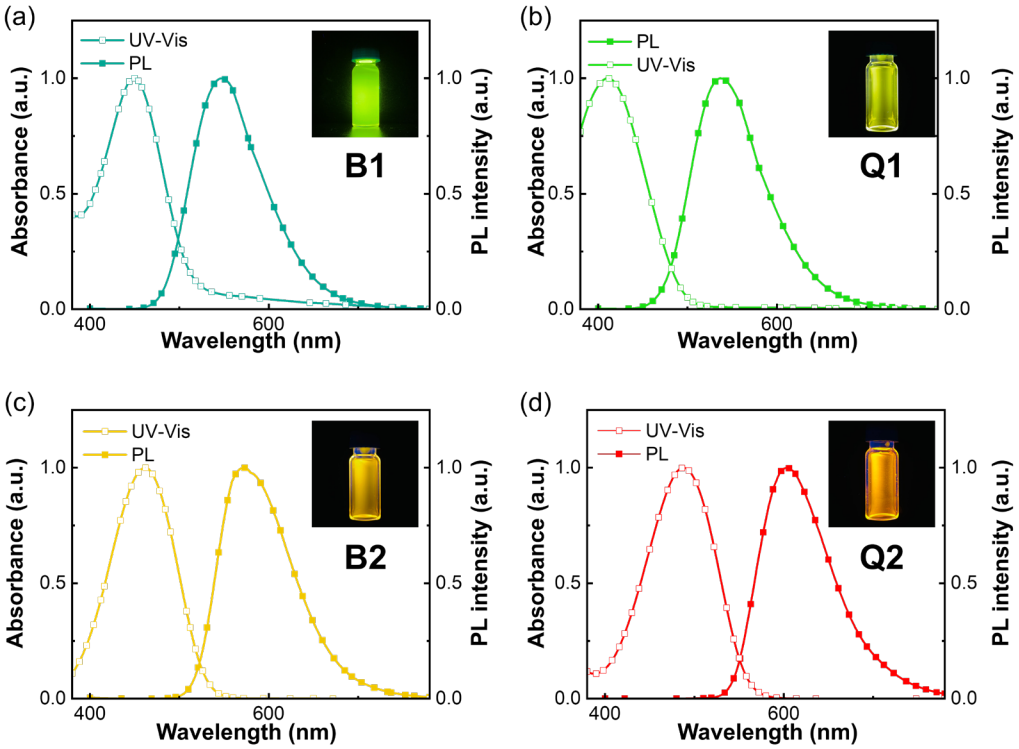

Fig. 2. UV-Vis absorption and steady-state PL spectra of broad-spectrum organic fluorescent small molecules. Inset: Fluorescent small molecule in DMSO solution at 365 nm UV light.

3.3 Electroluminescence (EL) properties

The energy level difference between the HOMO and LUMO of the luminescent material is a crucial factor in determining the OLED device structure and the choice of transmission layer material. The HOMO energy level of the device was obtained by ultraviolet photoelectron spectroscopy (UPS) and the E_g of small molecules was calculated from absorption spectra(Fig. S14 - S17).Subsequently, the LUMO energy level of the device was determined using the equation LUMO = HOMO + E_g, as shown in Fig. 3a. The results indicate that the HOMO energy levels of the emitter small molecules vary between -5.68 to -5.41 eV, while the LUMO energy levels of the devices range from -3.34 to -3.11 eV. The deep HOMO energy level of small molecule emitters is not conducive to carrier injection. Therefore, it is necessary to design a reasonable device structure to ensure optimal luminescence performance.

To evaluate the EL performances of the wide-spectrum emitters as the emissive layer (EML), solution-processed devices were fabricated with a simple configuration of ITO/PEDOT: PSS/EML/TPBi (30 nm)/LiF (0.5 nm)/Al (100

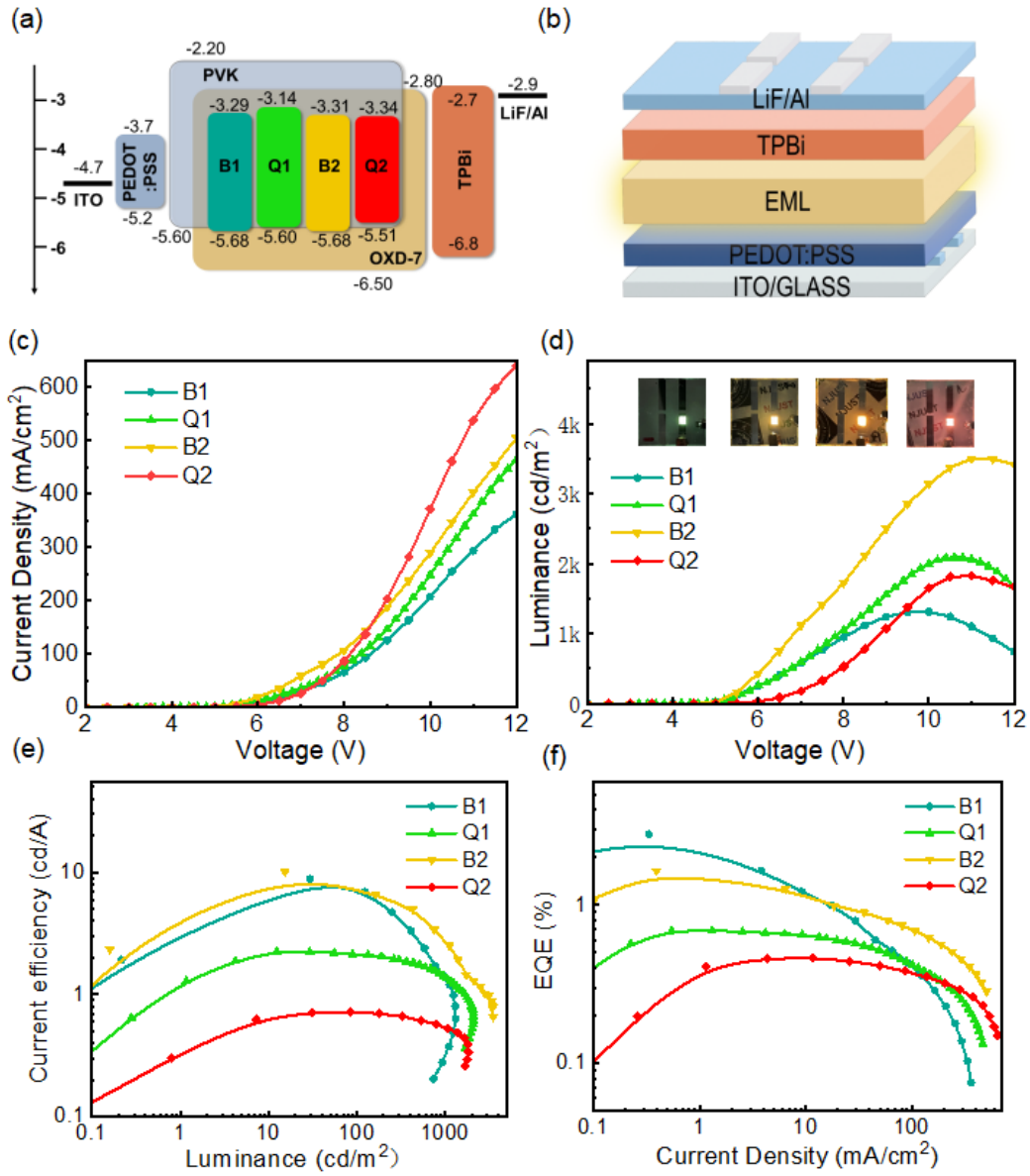

Fig. 3. (a) Energy level diagram of OLED with four different fluorescent luminescent small molecules. (b) Device structure diagram. (c) Current density−voltage characteristics of these OLEDs. (d) Luminance−voltage characteristics. Inset: showing four organic π-conjugated trimers OLEDs in work. (e) Current efficiency (CE) characteristics. (f) External quantum efficiency versus current density of these devices.

nm) (Fig. 3a-b). The anode, hole injection layer (HIL), electron transporting layer (ETL), and cathode used in all devices were ITO, PEDOT: PSS, TPBi, and LiF/Al, respectively. To further optimize the devices, host material was introduced to the EML to facilitate Förster energy transfer from the host to the fluorescent emitters.[41-46] Such as poly(N-vinyl carbazole) (PVK) with high triplet energy (-2.8 eV), 1,3-bis(5-(4-(tert-butyl)phenyl)-1,3,4-oxadiazol-2-yl) benzene (OXD-7) with deep HOMO level (-6.3 eV).[47-49] In this work, they were used as host materials to enhance the carriers' injection, the weight ratio of PVK to OXD-7 was 7:3. The morphology of the prepared film is shown in Fig. S18 - S21 in the

Supporting Information. The AFM images and height profile variations indicate that the thin films formed by the small molecules have minimal surface undulation and low roughness, confirming the compactness of the films, which helps to prevent carrier leakage and enhance the device's emission performance.

The performance characteristics of OLED devices and the key parameters of the devices are shown in Fig. 3c and Table 1, respectively. Specifically, these devices can generally achieve a luminance of more than 1000 cd m^{-2} (Fig. 3c-d).And the **B2**-based device (III) exhibits the best EL performance with a maximum EQE of 1.7%, a maximum luminance of 3499.21 cd m^{-2}, and a turn-on voltage (V_{ON}) of 4.89 V. Device B1 exhibits the highest EQE (2.8%) and a maximum luminance of 1313.59 cd m^{-2} compare with the other small molecules. In contrast, the **Q2**-based device (IV) exhibits a low EQE of 0.46%, but a higher luminance of 1826.08 cd m^{-2} (Fig. 3e-f).

The maximum EQE of the **B1** and **B2** based devices (I and III) is attributed to the effective carrier confinement within the EML. This indicates that organic light-emitting small molecules constructed based on 2,1,3-Benzothiadiazole centers have a superior ability to bind charges and holes, thereby promoting better light-emitting properties.

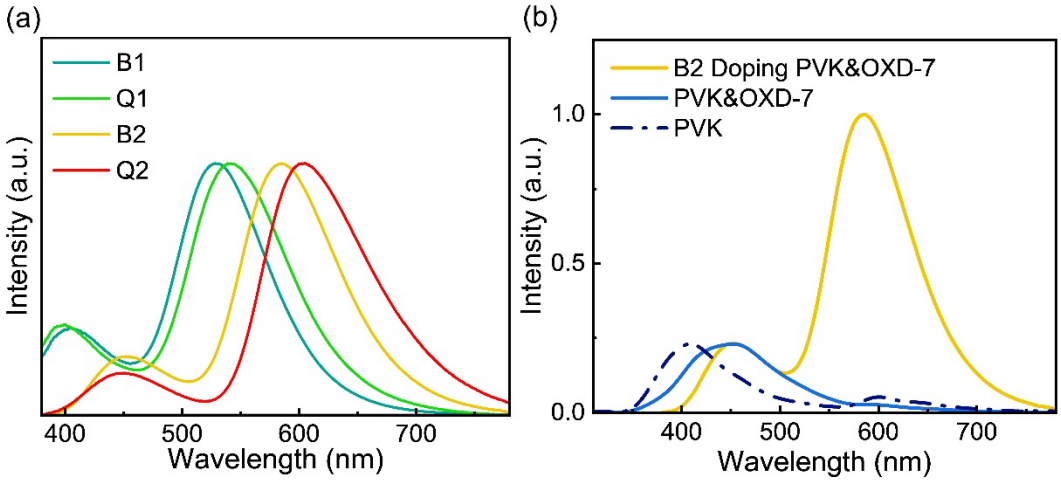

Fig. 4. Luminous spectrum. (a) Electroluminescence spectrum of the devices. (b) Electroluminescence spectra of devices with the structure: ITO/PEDOT:PSS/PVK or PVK & OXD-7 or **B2** doping PVK & OXD-7/TPBi/LiF/Al.

Photoluminescence spectra of **B1**, **Q1**, **B2**, and **Q2** and the devices (I-VI) demonstrates a strong emission with EL peaks (λ_{EL}) at 528 nm (**B1**), 539 nm (**Q1**), 585 nm (**B2**) and 605 nm (**Q2**) (Fig. 4a). The EL spectra were well matched with the PL spectra and their EL peaks did not drift with different voltages, indicating the stability of the carrier injection and recombination (Fig. S22), further promotes the stability of CIE coordinates (Fig. S23). It is worth noting that the **B1** and **Q1** devices show a sub-peak at 410 nm, which corresponds to the well-known PVK emission peak of hole transport layer materials. Nevertheless, the EL spectra of the **B2** and **Q2** devices reveal a low luminescence at 450 nm, which is not consistent with the PVK peak (410 nm)[47] or the OXD-7 peak (330 nm).[48, 50] This emission is probably caused by interfacial emission, implying that a portion of the electron-hole recombination occurs at the interface of the hole transport materials, leading to the dark blue fluorescence of the device. To investigate this, we fabricated devices featuring a single hole transport layer of PVK and a mixed layer combining PVK and OXD-7(Fig. 4b). The EL peak of the single PVK transport layer is observed at 408 nm, accompanied by an exciton complex peak at 600 nm. As shown in Figure S22, the brightness of PVK emission continues to increase with applied voltage, while the exciplex emission

remains relatively unchanged. This is because the energy level of the exciplex is determined by the interaction between PVK and TPBi and saturates at low voltage. In contrast, the higher energy level of PVK makes it harder to saturate at low voltage, leading to a continuous increase in brightness as the carrier injection increases with voltage. In contrast, the hybrid transport layer device exhibits a lower-intensity exciton complex peak at 600 nm, overshadowed by the peak at 450 nm. This elucidates the origin of the 450 nm peak observed in the prepared OLED.

Table 1. Electroluminescent data of wide-spectrum OLED devices

Device[a]	EML	V_{ON}[b]	L_{max}[c] (cd m^{-2})	J_{max}[d] （mA cm^{-2}）	λ_{EL}[e] (nm)	FWHM[f] (nm)	EQE_{max}[g] at voltage (%, V)	CIE[h]
Ⅰ	**B1**	4.62	1313.59	362.15	528	92	2.80/5	(0.39, 0.48)
Ⅱ	**Q1**	4.38	2089.47	465.19	539	100	0.69/5	(0.34, 0.48)
Ⅲ	**B2**	4.89	3499.21	505.04	585	98	1.7/5.5	(046,0.42)
Ⅳ	**Q2**	5.05	1826.08	641.55	605	108	0.46/6.5	(0.52, 0.36)

[a] ITO/PEDOT: PSS/EML/TPBi (30 nm)/LiF (0.5 nm)/Al (100 nm)

[b] Turn on voltage at 1 cd m^{-2}.

[c]Maximum luminance.

[d] Maximum current.

[e] Emission maximum.

[f]Full width at half maximum.

[g]Maximum external quantum efficiency.

[h] Commission Internationale de l'éclairage coordinates (x, y).

3.4 Small molecule LED molecular weight comparison

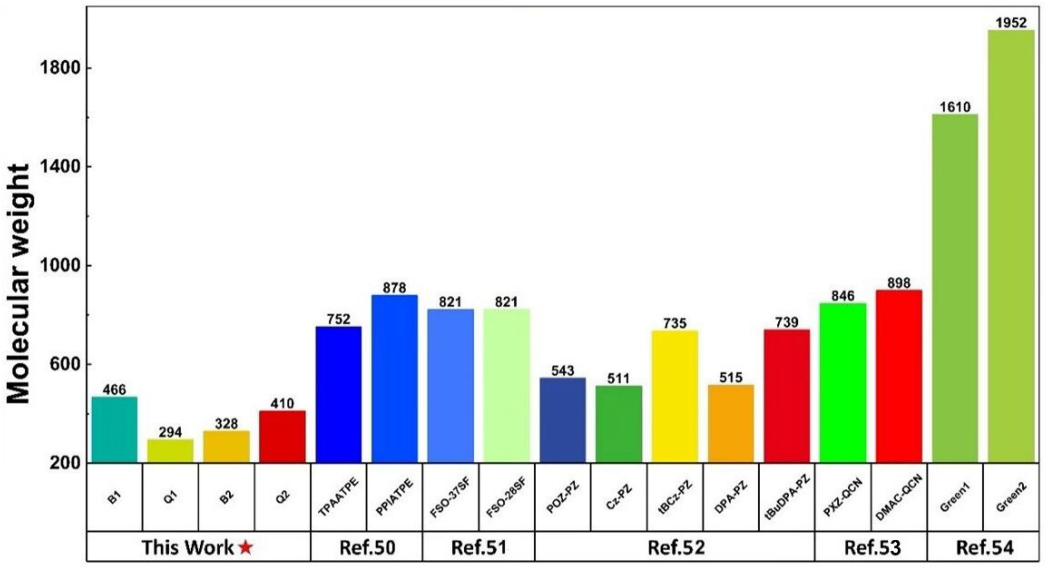

Fig. 5. Comparison of molecular weight of different small molecule organic light-emitting materials.

These small molecules possess exceedingly simple structures with ultra-small molecular weights, while they exhibit outstanding luminescent properties. Their precise molecular structure allows for enhanced control over both physical and electronic properties. This feature enables precise tuning of emission wavelength, energy efficiency, and stability, making them ideal for the production of bright and durable OLEDs.[49, 51] Organic π-conjugated trimers with D-A-D structure possess molecular weights of merely 294 - 466, significantly smaller than other molecules.[52-55] For instance, blue molecules consisting of triphenylamine/phenanthroimidazole and tetraphenylethene-substituted anthracene(M_w=752-878), orange-red thermally activated delayed fluorescence molecules of quinoxaline (M_w=846-898), and green organic molecules based on the benzothiadiazole core (M_w=1610-1952), as shown in Fig. 5. Furthermore, we successfully implemented solution processing for ultra-small molecules, significantly reducing both materials and equipment costs in device manufacturing.

4. Conclusion

In conclusion, a series of organic π-conjugated trimers based on carbazole, thiophene, 3,4-ethylenedioxythiophene, quinoxaline and 2,1,3-benzothiadiazole units have been designed, exhibiting great potential in OLED applications. By doping with PVK and OXD-7, these solution-processed devices show stable and high luminescence (up to3500 cd m^{-2}). With the lowest molecular weight and excellent solution processing capability, these conjugated trimers displayconsiderable potential for the development of low-cost OLEDs.

Conflicts of interest

The authors declare no competing financial interest.

Acknowledgements

The authors gratefully acknowledge financial support by National Key Research and Development Program of China (2022YFB3606502); National Natural Science Foundation of China (52131304，62004101); The Excellent Talents Program of HYNU.

Author contributions

Yanhong Deng: Methodology, Validation, Investigation, Writing − review & editing, Formal analysis. Validation, Investigation, **Yifei Wang：** Methodology, Validation, Investigation, Writing − original draft. **Zhesheng Chen**: Investigation. **Bo Xu**: Investigation. **Jinjiang Wang:** Supervision. **Eric Cloutet:** Supervision, Investigation. **XiaojiaoYuan:** Conceptualization, Formal analysis, Writing − review & editing. **Hengyang Xiang:** Funding acquisition; Supervision; Writing − review & editing.

References

1 Q. Xu, S. Zhou, J. Huang, X. Ouyang, J. Liu, Y. Guo, J. Wang, J. Nie, X. Zhang, X. Ouyang and W. Jia, *Materials Today Physics*, 2021, **18**.
2 Y. Liu, C. Li, Z. Ren, S. Yan and M. R. Bryce, *Nature Reviews Materials*, 2018, **3**.
3 X. Li, X. Gao, W. Shi and H. Ma, *Chemical Reviews*, 2014, **114**, 590-659.
4 H. Kim, W. Park, Y. Kim, M. Filatov, C. H. Choi and D. Lee, *Nat Commun*, 2021, **12**, 5409.

5 Y. Wang, H. Wu, W. Hu and J. F. Stoddart, *Adv Mater*, 2022, **34**, e2105405.
6 H. Sasabe and J. Kido, *Chemistry of Materials*, 2010, **23**, 621-630.
7 L. Duan, J. Qiao, Y. Sun and Y. J. A. M. Qiu, 2011, **23**, 1137-1144.
8 Y. Hong, J. W. Lam and B. Z. Tang, *Chem Soc Rev*, 2011, **40**, 5361-5388.
9 S. Wang, X. Yan, Z. Cheng, H. Zhang, Y. Liu and Y. Wang, *Angewandte Chemie*, 2015, **127**, 13260-13264.
10 Y. Liu, X. Xiao, Y. Ran, Z. Bin and J. You, *Chem Sci*, 2021, **12**, 9408-9412.
11 A. C. Tadle, K. A. El Roz, C. H. Soh, D. Sylvinson Muthiah Ravinson, P. I. Djurovich, S. R. Forrest and M. E. Thompson, *Advanced Functional Materials*, 2021, **31**.
12 H. Usta, D. Alimli, R. Ozdemir, S. Dabak, Y. Zorlu, F. Alkan, E. Tekin and A. Can, *ACS Appl Mater Interfaces*, 2019, **11**, 44474-44486.
13 X. Chen, H. Xiang, R. Wang, Y. Wang, Y. Wang and H. Zeng, *Advanced Functional Materials*, 2023, **33**, 2304750.
14 R. Wang, H. Xiang, Y. Li, Y. Zhou, Q. Shan, Y. Su, Z. Li, Y. Wang and H. Zeng, *Advanced Functional Materials*, 2023, **33**, 2215189.
15 A. Dhara, T. Sadhukhan, E. G. Sheetz, A. H. Olsson, K. Raghavachari and A. H. Flood, *J Am Chem Soc*, 2020, **142**, 12167-12180.
16 A. N. Butkevich, G. Lukinavicius, E. D'Este and S. W. Hell, *J Am Chem Soc*, 2017, **139**, 12378-12381.
17 J. B. Grimm, A. K. Muthusamy, Y. Liang, T. A. Brown, W. C. Lemon, R. Patel, R. Lu, J. J. Macklin, P. J. Keller, N. Ji and L. D. Lavis, *Nat Methods*, 2017, **14**, 987-994.
18 R. Lincoln, M. L. Bossi, M. Remmel, E. D'Este, A. N. Butkevich and S. W. Hell, *Nat Chem*, 2022, **14**, 1013-1020.
19 X. Liu, Q. Qiao, W. Tian, W. Liu, J. Chen, M. J. Lang and Z. Xu, *J Am Chem Soc*, 2016, **138**, 6960-6963.
20 C. Wang, W. Chi, Q. Qiao, D. Tan, Z. Xu and X. J. C. S. R. Liu, 2021, **50**, 12656-12678.
21 Z. Xie, C. Chen, S. Xu, J. Li, Y. Zhang, S. Liu, J. Xu and Z. Chi, *Angewandte Chemie*, 2015, **127**, 7287-7290.
22 Z. Ma, M. Teng, Z. Wang, S. Yang and X. Jia, *Angew Chem Int Ed Engl*, 2013, **52**, 12268-12272.
23 M. Guo, Y. Lu, X. Cai, Y. Shen, X. Qian, H. Ren, Y. Li, W. Wang and J. Tang, *Journal of Materials Chemistry C*, 2022, **10**, 2998-3005.
24 F. Ni, Z. Wu, Z. Zhu, T. Chen, K. Wu, C. Zhong, K. An, D. Wei, D. Ma and C. Yang, *Journal of Materials Chemistry C*, 2017, **5**, 1363-1368.
25 T. Kaewpuang, C. Chaiwai, P. Chasing, P. Wongkaew, T. Sudyoadsuk, S. Namuangruk, T. Manyum and V. Promarak, *Journal of Photochemistry and Photobiology A: Chemistry*, 2021, **420**.
26 L. Yu, Z. Wu, G. Xie, C. Zhong, Z. Zhu, D. Ma and C. Yang, *Chem Commun (Camb)*, 2018, **54**, 1379-1382.
27 P. Ledwon, R. Motyka, K. Ivaniuk, A. Pidluzhna, N. Martyniuk, P. Stakhira, G. Baryshnikov, B. F. Minaev and H. Ågren, *Dyes and Pigments*, 2020, **173**.
28 V. Yeddu, G. Seo, F. Cruciani, P. M. Beaujuge and D. Y. Kim, *ACS Photonics*, 2019, **6**, 2368-2374.
29 C. Zhou, X. Zhang, G. Pan, X. Tian, S. Xiao, H. Liu, S. Zhang and B. Yang, *Organic Electronics*, 2019, **75**.
30 W. W. H. Lee, Z. Zhao, Y. Cai, Z. Xu, Y. Yu, Y. Xiong, R. T. K. Kwok, Y. Chen, N. L. C. Leung, D. Ma, J. W. Y. Lam, A. Qin and B. Z. Tang, *Chem Sci*, 2018, **9**, 6118-6125.
31 Y. Zhou, M. Zhang, J. Ye, H. Liu, K. Wang, Y. Yuan, Y.-Q. Du, C. Zhang, C.-J. Zheng and X.-H. Zhang, *Organic Electronics*, 2019, **65**, 110-115.
32 Y. C. Lo, T. H. Yeh, C. K. Wang, B. J. Peng, J. L. Hsieh, C. C. Lee, S. W. Liu and K. T. Wong, *ACS Appl Mater Interfaces*, 2019, **11**, 23417-23427.
33 T. Huang, D. Liu, J. Jiang and W. Jiang, *Chemistry*, 2019, **25**, 10926-10937.
34 P. Zassowski, P. Ledwon, A. Kurowska, A. P. Herman, M. Lapkowski, V. Cherpak, Z. Hotra, P. Turyk, K. Ivaniuk, P. Stakhira, G. Sych, D. Volyniuk and J. V. Grazulevicius, *Dyes and Pigments*, 2018, **149**, 804-811.
35 L. A. Lozano-Hernandez, J. L. Maldonado, C. Garcias-Morales, A. Espinosa Roa, O. Barbosa-Garcia, M. Rodriguez and E. Perez-Gutierrez, *Molecules*, 2018, **23**.

36 C. Kok, C. Doyranli, B. Canimkurbey, S. Piravadili Mucur and S. Koyuncu, *RSC Adv*, 2020, **10**, 18639-18647.
37 G. Turkoglu, M. E. Cinar, A. Buyruk, E. Tekin, S. P. Mucur, K. Kaya and T. Ozturk, *Journal of Materials Chemistry C*, 2016, **4**, 6045-6053.
38 G. Savitha, C. Moussallem, M. Allain, F. Gohier and P. Frere, *Chem Asian J*, 2017, **12**, 1935-1943.
39 H. Akpınar, A. Balan, D. Baran, E. K. Ünver and L. Toppare, *Polymer*, 2010, **51**, 6123-6131.
40 X. Yuan, C. Wang, L. Vallan, A. T. Bui, G. Jonusauskas, N. D. McClenaghan, C. Grazon, S. Lacomme, C. Brochon, H. Remita, G. Hadziioannou and E. Cloutet, *Advanced Functional Materials*, 2023, **33**.
41 Y. Ning, J. Yang, H. Si, H. Wu, X. Zheng, A. Qin and B. Z. Tang, *Science China Chemistry*, 2021, **64**, 739-744.
42 Y. Zhou, T. Fang, G. Liu, H. Xiang, L. Yang, Y. Li, R. Wang, D. Yan, Y. Dong and B. J. A. F. M. Cai, 2021, **31**, 2106871.
43 Q. Shan, Y. Dong, H. Xiang, D. Yan, T. Hu, B. Yuan, H. Zhu, Y. Wang and H. J. A. F. M. Zeng, 2024, 2401284.
44 J. Jiang, S. Zhang, Q. Shan, L. Yang, J. Ren, Y. Wang, S. Jeon, H. Xiang and H. J. A. M. Zeng, 2024, 2304772.
45 H. Fukagawa, T. Shimizu, Y. Iwasaki and T. Yamamoto, *Sci Rep*, 2017, **7**, 1735.
46 H. Xiang, R. Wang, J. Chen, F. Li and H. Zeng, *Light Sci Appl*, 2021, **10**, 206.
47 C.-J. Chang, Y.-Y. Cheng, M. H. Wang and C. S. Tuan, *Thin Solid Films*, 2005, **477**, 14-18.
48 J. Saghaei, S. M. Russell, H. Jin, P. L. Burn, A. Pivrikas and P. E. Shaw, *Advanced Functional Materials*, 2021, **32**.
49 N. Aizawa, Y. J. Pu, M. Watanabe, T. Chiba, K. Ideta, N. Toyota, M. Igarashi, Y. Suzuri, H. Sasabe and J. Kido, *Nat Commun*, 2014, **5**, 5756.
50 T. Xu, G. Xie, T. Huang, H. Liu, X. Cao, Y. Tang and C. Yang, *Organic Electronics*, 2021, **96**.
51 T. H. Han, M. R. Choi, C. W. Jeon, Y. H. Kim, S. K. Kwon and T. W. Lee, *Sci Adv*, 2016, **2**, e1601428.
52 F. Liu, H. Liu, X. Tang, S. Ren, X. He, J. Li, C. Du, Z. Feng and P. Lu, *Nano Energy*, 2020, **68**.
53 L. Hu, N. Wang, D. Chen, S.-J. Su, W. Yang and B. Zhang, *Journal of Photochemistry and Photobiology A: Chemistry*, 2019, **382**.
54 M. Xie, J. Cai, X. Wang, T. Shan, S. Jung, H. Zhong, X. Guo, D. Zhou and T. Li, *Advanced Optical Materials*, 2022, **10**.
55 N. J. Findlay, B. Breig, C. Forbes, A. R. Inigo, A. L. Kanibolotsky and P. J. Skabara, *Journal of Materials Chemistry C*, 2016, **4**, 3774-3780.